



This is to certify that the

thesis entitled

Control of Thermal Conductivity in Electrorheological (ER) Fluid Composite Materials

presented by

Yinxue Su

has been accepted towards fulfillment of the requirements for

M.S. degree in Mechanical Engineering

O-7639

Date August 21, 199 f

MSU is an Affirmative Action/Equal Opportunity Institution

LIBRARY Michigan State University

PLACE IN RETURN BOX to remove this checkout from your record.

TO AVOID FINES return on or before date due.

DATE DUE	DATE DUE	DATE DUE

MSU Is An Affirmative Action/Equal Opportunity Institution cycle/datedus.pm3-p.1

CONTROL OF THERMAL CONDUCTIVITY IN ELECTRORHEOLOGICAL (ER) FLUID COMPOSITE MATERIALS

by

Yinxue Su

A THESIS

Submitted to
Michigan State University
in partial fulfillment of the requirements
for the degree of

MASTER OF SCIENCE

Department of Mechanical Engineering

ABSTRACT

CONTROL OF THERMAL CONDUCTIVITY IN ELECTRORHEOLOGICAL (ER) FLUID COMPOSITE MATERIALS

By

Yinxue Su

A theoretical model that incorporates the thermal properties and electrical properties with the ER effect is presented. The thermal conductivity of the isotropic ER fluid is measured and the effect of temperature on the thermal conductivity is investigated adopting a transient method. A new approach that is defined as internal heat generation technique has been proposed and the thermal conductivity for the chain structured ER fluid is successfully measured using this new method. The experimental results have demonstrated that the water content and the temperature are the dominant factors controlling the thermal conductivity of the ER fluid exposed to electric field. A high thermal conductivity will be resulted if strong chaining can be established at low temperatures.

ACKNOWLEDGMENTS

I would like to express my gratitude to my advisor, Dr. John R. Lloyd for his thoughtful and patient guidance throughout my graduate program. I am deeply impressed by his excellent guidance and his great personality. My master's committee members, Dr. Andre Benard and especially Dr. Clark Radcliffe who provided me with both equipment and patient guidance will always have my sincere thanks.

My thanks go to the other members of our team that gave me their assistance and their friendship, especially Gloria Elliott and Omar Hayes for their help. I would also like to thank Craig Gunn for his help with the improvement of my writing skill and with the writing guide for this thesis.

TABLE OF CONTENTS

LIS	T OF TABLES	vi
LIS	T OF FIGURES	vii
NO	MENCLATURE	ix
1	INTRODUCTION	1
2	ANALYSIS	5
	ER FLUIDS WITH ZERO ELECTRIC FIELD	
	ER FLUIDS EXPOSED TO AN ELECTRIC FIELD	8
	The Energy Distribution	8
	Equations for the Electric Field	
	Temperature Field Resulted from Joule Heat of a Single Sphere	
3	EXPERIMENTAL APPARATUS AND TECHNIQUE	20
	HOMOGENOUS ER FLUIDS	20
	Experimental Apparatus	20
	ER Materials and Their Properties	
	Experimental Procedure	
	CHAIN STRUCTURED ER FLUIDS	
	Transient Technique	
	Internal Heat Generation Technique	
	Theoretical Background	
	Experimental Procedure	29
4	RESULTS AND DISCUSSIONS	31
	SILICONE OIL AND ZEOLITE PARTICLE CALIBRATION	31
	HOMOGENOUS ER FLUIDS	32
	Comparison Between Prediction and Measurement	32
	Temperature Effect	
	CHAIN STRUCTURED ER FLUIDS	36
	Results from Transient Technique	36
	Results from Internal Heat Generation Technique	37
	ER Phenomenon	37
	Thermal Conductivity	42
5	CONCLUDING REMARKS	50

BIBLIOGRAPHY	52
APPENDIX A	56
APPENDIX B	59

LIST OF TABLES

- Table 1 Characteristics of Components of the Composite Specimen
- Table 2 Thermal Conductivity of ER Fluid as a Function of Applied Electric Field ($f_v = 35\% H_2O \text{ wt.8\%}$)
- Table 3 Thermal Conductivity, λ of ER Fluid as a Function of Applied Electric Field ($f_v = 10\% H_2O \text{ wt.}19\%$)
- Table 4 List of Available ER Fluids
- Table 5 General Characteristics of ER Fluids (Gast and Zukoski 1989)
- Table 6 Data for Fig.8
- Table 7 Data for Fig.9
- Table 8 Data for Fig.10
- Table 9 Values of Parameters and Their Variations

LIST OF FIGURES

- Fig. 1. Chain Structure of Zeolite/Silicone Oil Exposed to Electric Field
- Fig. 2. Effect of Ratio of Particle-Fluid Thermal Conductivity on the Temperature Field Around a Particle
- Fig. 3. Effect of Ratio of Particle-Fluid Dielectric Constant on the Temperature Field Around a Particle
- Fig. 4. Ratio of Particle-Fluid Dielectric Constant vs Temperature (Data from Conrad et al, 1991)
- Fig. 5. Experimental Setup to Measure the Thermal Conductivity of Isotropic ER Fluid
- Fig. 6. Experimental Setup to Measure the Thermal Conductivity of ER Fluid With Electric Field
- Fig. 7. Schematic of Temperature Field in Half of the Symmetry ER Assembly
- Fig. 8. Thermal Conductivity of Silicone Oil
- Fig. 9. Thermal Conductivity of Zeolite/Silicone Oil Suspensions
- Fig. 10. Temperature Effect on the Thermal Conductivity, λ of Isotropic ER Fluid
- Fig. 11. Electric Property Response of ER Fluid with Low Electric Field and High Water Content
- Fig. 12. Electric Property Response of ER Fluid with Low Electric Field and Low Water Content
- Fig. 13. Electric Property Response of ER Fluid with High Electric Field and High Water Content
- Fig. 14. Typical Temperature Profile of ER Fluid Exposed to Electric Field
- Fig. 15. Temperature Fluctuation of ER Fluid at High Electric Field
- Fig. 16. Dependence of the ER Effect on the Initial States

- Fig. 17. Transient Temperature Profiles for T and $(T-T_J)$ at Positions of z=0 and z=L
- Fig. 18. A Correction to the Thermal Conductivity of the Structured ER Fluid with Consideration of Joule Heat
- Fig. 19. Temperature Profile of ER Fluid at High Electric Field
- Fig. 20. Joule Heat and Electric Conductivity of ER Fluid at High Electric Field

NOMENCLATURE

Arabic Symbols

a = radius of particle

 C_p = specific heat capacity

D = diameter of the electrode plate

D = electric induction vector

e = exponential function

E = electric field vector

E = scalar electric field, kV/mm

 f_v = particle volume fraction

j = current density, A/m²

 K_e = effective thermal conductivity, $K_e = \frac{\lambda}{\lambda_f}$

L = the thickness of ER fluid layer, mm

q = Joule heat, kW/m^3

 q_s = surface heat flux, W/m²

m = empirical coefficient in equation (2.3)

r = radius, m

r = radius vector

R = dimensionless radius, $R = \frac{r}{a}$

 $T = temperature (^{\circ}C)$

t = time

V = voltage

X = sensitivity coefficient

z = the coordinate along the direction of electric field in ER fluid sample

Greek Symbols

 α = thermal diffusive coefficient

 β = dielectric mismatch parameter, $\beta = \frac{\varepsilon_p - \varepsilon_f}{\varepsilon_p + 2\varepsilon_f}$

 β_1 = ratio of dielectric constant, $\beta_1 = \frac{\varepsilon_p}{\varepsilon_f}$

 β_2 = ratio of thermal conductivity, $\beta_1 = \frac{\lambda_p}{\lambda_f}$

 γ = angle between r and E

 ε = dielectric constant

 λ = thermal conductivity, W/mK

 θ = dimensionless temperature, $\theta = \frac{T - T_{\infty}}{E^2 \sigma_p a^2 / \lambda_p}$

 ρ = density

 σ = electric conductivity, S/m

Subscript

- p particle
- f fluid
- J Joule heat

1 INTRODUCTION

Electrorheological (ER) fluids, are a member of the class of smart, intelligent, or controllable fluids, and consist of a suspension of fine dielectric particles in a liquid of low dielectric constant. ER fluids can have variable rheological, electrical, optical, thermal, volumetric, and acoustic properties based on the character of the microstructure of the fluid when controlled by the application of an electric field.

Since the discovery of this ER phenomenon by Willis M. Winslow (1947), researchers have attempted to model the properties of ER fluids and have proposed numerous applications that attempt to utilize their special characteristics. Such applications include the operation of active suspension systems, vibration control systems, hydraulic valves, and transmission systems. Most of these applications are based on utilizing the controllable rheological property of ER fluid viscosity to engineer systems where variable viscosity is desired. Examples of these applications include automotive engine mounts (Hartsock et al. 1991, Petek et al. 1989, Williams et al. 1993), vibration control devices (Coulter and Duclos 1989, Hartsock et al. 1991), variable torque transmissions (Carlson 1989), dampers (Li et al. 1995, Morishita et al. 1995), and brakes and clutches (Carlson and Duclos 1989). And the heat transfer application of ER fluids

2

began with Shulman's early work (1982) where the ER fluids were utilized as a working medium for a heat exchanger.

Numerous papers have recently been published concerning the state of the art of ER fluid research and application. For example, a recent review can be found in the work of Filisko (1995) and that of Block and Rattray (1995). Recent literature indicates that many theories have been proposed to explain the ER effect, including the classical Maxwell-Wagner-Sillars (MWS) interfacial polarization theory, the water bridging theory (Stangroom 1983), the electrical double layer theory (Klass and Martinek 1967a, 1967b), and theories that focus on the intrinsic chemistry and mechanisms of the ER materials responsible for the ER activity. All of these works are aimed at enabling the design and improvement of ER fluid performance in regard to commercial applications.

However, the commercialization of this promising technology is still hampered by the lack of understanding of the materials and the mechanisms responsible for the ER effect. The application of ER fluids in heat transfer control is even more elusive, due to the poor understanding of the heat transfer mechanism associated with the ER phenomena. The objective of the present work is to provide some insight into the physical mechanism from the thermal aspect associated with ER effect.

Recently, interest in the area of control of the thermal properties of ER fluids has increased. Upon application of an electric field, the particles in ER fluids form chains between the two electrodes along the lines of the electric field and create preferred pathways for energy transport. The micro-structure transitions result in changes in the macro thermal transport properties such as thermal conductivity, convective heat transfer

3

coefficient, and radiate heat transfer transport. ER fluids provide a novel way to control heat transfer processes.

There has been a very limited amount of research done on this novel concept, and that has been accomplished by Shulman and his coworkers (Shulman 1982, Shulman et al. 1986, Korobko 1992) at the Luikov Institute of Heat and Mass Transfer in Minsk, and by Lloyd and Radcliffe and their research group (Lloyd and Zhang 1992 a, b, 1993, 1994, Hargrove 1997, Elliott 1997, McGregor 1997, Omar 1997) at Michigan State University.

In Shulman's work (1982), the ER fluid was composed of diatomaceous earth and transformer oil, which have a thermal conductivity of 0.126 and 0.144 W/mK, respectively. It is obvious that by linearly mixing these two phases, the maximum thermal conductivity should not be larger than 0.144 W/mK. But they found up to a three-fold increase of the thermal conductance of this particular ER fluid over the value of 0.144 W/mK with application of a strong electric field. What is the reason behind the 300% increase? Is this phenomenon repeatable?

Lloyd and his group are involved in an extensive research program to explore the applications of ER fluids in thermal control areas. In one of those works, Zhang and Lloyd (1993) have demonstrated a 55% increase in apparent thermal conductivity with the application of a strong electric field.

In thermal control applications, it is obvious that temperature is a very important property to take into account, especially the effect of temperature on the properties of ER material. Nelson and Suydam (1993) have advanced to the complexity of investigating the temperature effect on the viscosity and concluded that the viscosity decreased as the

temperature increased, characterizing the fluid as temperature thinning. And in the work of Conrad et al. (1991) and Conrad and Chen (1995), the temperature dependence of the electrical properties and chaining strength of electrorheological fluids have been investigated. They found that the strength of the chaining of the ER fluid increases with increasing temperature, and there appears to be an upper temperature limit for the increase in strength (occurs 120 - 150°C). The electrical conductivity and dielectric constant of the particles increase with the temperature while the dielectric constant of the silicone oil decreases slightly with temperature. They suggested that the increase of the conductivity and dielectric constant of the suspension stems from the diffusion of Na+ions in the zeolite particles as well as from the mobile charge carriers whose number or mobility are thermally activated. There is no available information about the influence of temperature on the thermal properties of ER material.

The present work focuses on the investigation of the physical mechanisms of ER activity, especially in the thermal aspect. Theoretical analysis of the thermal conduction process in the ER phenomenon will be performed and a new measurement technique for the thermal conductivity will be presented. The measured results using different techniques will be discussed.

2 ANALYSIS

It is appropriate to discuss here the general mechanism of thermal conduction in fluids. When a temperature gradient is applied to a liquid for which a lattice structure is assumed, the excess energy between layers transported down the gradient is transported by convective and vibration mechanisms. Convective transport is accomplished through the motion of molecules. While energy transport by vibration mechanism is the intracellular and collisional contribution with the origin in the intermolecular forces. It is found that the convective term is negligible compared with the intermolecular force contribution (McLaughlin 1959). A higher thermal conductivity λ can be expected with higher intermolecular forces.

The energy transport mechanism should be different for the ER fluid with randomly distributed particles as compared to an ER fluid with chained particles. These two states of particle organization and their effective thermal energy transport will be analyzed in the following sections.

ER FLUIDS WITH ZERO ELECTRIC FIELD

In the absence of an electric field, the suspension is taken to be a continuous medium with particles randomly oriented. For such a system, a statistical method for calculating the average properties of the suspension (Khusid and Acrivos 1995, Shulman et al. 1982) may be used.

The equation developed by Shulman (1982) for metal-filled systems will be adopted here to predict the effective thermal conductivity of the ER suspension. He proposed the following

$$\frac{\lambda_e - \lambda_f}{\lambda_e + 2\lambda_f} = f_v \frac{\lambda_p - \lambda_f}{\lambda_p + 2\lambda_f} \tag{2.1}$$

This equation coincides with a similar equation for the derivation of the Maxwell-Wagner expression for the permittivity of a suspension (Dukhin and Shilov 1974):

$$\frac{\varepsilon_{e} - \varepsilon_{f}}{\varepsilon_{e} + 2\varepsilon_{f}} = f_{i} \frac{\varepsilon_{p} - \varepsilon_{f}}{\varepsilon_{p} + 2\varepsilon_{f}}$$
(2.2)

This suggests that a relationship may exist between thermal conductivity and electrical phenomena.

Similarly, Hamilton and Crosser (1963) suggested an empirical relationship for the thermal conductivity of the medium with randomly dispersed particles

$$\frac{\lambda_e - \lambda_f}{\lambda_e + (m-1)\lambda_f} = f_v \frac{\lambda_p - \lambda_f}{\lambda_p + (m-1)\lambda_f}$$
(2.3)

where m is an empirical coefficient accounting for the anisodiametricity of the particles.

Also more involved models have been developed for the prediction of the effective thermal conductivity of such kinds of system. Depending on the ratio of the individual phase conductivity, the models are based on two categories of assumptions. One is to assume linear heat flow (for the case of $\beta_2 \sim 1$), and the other is to assume nonlinear flow (for the case of $\beta_2 >>1$ or $\beta_2 <<1$).

Based on the linear assumption, the following equation developed by Jefferson et al. (1958) is selected:

$$K_{e} = 1 - \frac{\pi}{4(1+2n)^{2}} + \frac{\pi}{4(1+2n)^{2}} \frac{(0.5+n)K_{a}}{0.5+nK_{a}}$$
(2.4)

where

$$K_a = \beta_2 \frac{2\beta_2}{(\beta_2 - 1)^2} \ln \beta_2 - \frac{2}{\beta_2 - 1}$$
$$n = 0.403 f_y^{-2/3} - 0.5$$

This is valid for particle volume concentration $f_v < 0.52$.

Based on the nonlinear assumption, an expression for effective thermal conductivity accounting for this interaction for uniform size spheres in a cubic lattice

arrangement was derived by Rayleigh (1892). He used a second - order treatment accounting for dipoles and octupoles only and his result is shown below

$$K_{\epsilon} = 1 - 3f_{\nu} \left[\frac{2 + \beta_{2}}{1 - \beta_{2}} + f_{\nu} - \frac{0.525(1 - \beta_{2})f_{\nu}^{10/3}}{4/3 + \beta_{2}} \right]^{-1}$$
 (2.5)

This equation is valid for particle volume concentrations $f_v < 0.5236$, and it is assumed that the particles are uniform spheres.

Prediction from these empirical equations will be compared to the measured effective thermal conductivity of the Zeolite / Silicone Oil suspension.

ER FLUIDS EXPOSED TO AN ELECTRIC FIELD

The Energy Distribution

It is well known that upon application of an electric field, the particles align into a chain-like or fibrous structure roughly parallel to the field. (An example of the ER effect of Zeolite / Silicone Oil suspension with $f_v = 5\%$ and E = 1.5 kV/mm is shown in Fig. 1). This unique structure transition from isotropic to nonisotropic, referred as the "Winslow effect", is the key to controlling the directional thermal conductivity since it has created preference pathways for the energy transport. From a macroscopic point of view, the electrostatic energy of a system of charged conductor or dielectric has been defined as

$$W = \frac{1}{2} \int_{V} D \cdot E dV \tag{2.6}$$



Fig. 1. Chain Structure of Zeolite / Silicone Oil Exposed to Electric Field

Khusid and Acrivos (1996) concede that in the case of non-conducting particles and liquids, the electrostatic energy of a suspension is determined completely by its dielectric constant and the particle concentration f_v . This electrostatic energy includes the various self-energies of the suspensions and the interaction energies to bring the particles into chaining state and to maintain the ordered structure (Reitz 1967). This highly ordered ER fluid, which is exposed to the external electric field, has lower entropy than that without electric field. According to the second law of thermodynamics, the decrease in entropy of a system has to be accompanied with energy dissipation, i.e. the structured ordering of the ER suspension occurs at a cost in the energy loss. By Joule's law, the heat loss in the process is

$$q = j \cdot E \tag{2.7}$$

The total internal energy of the system is physically meaningful associated with the microstructure transition when the fluid is exposed to electric field. To relate the electrostatic energy and the heat loss to the total internal energy of the system, let us look at the first law of thermodynamics for a reversible process

$$du_i = Tds + dw (2.8)$$

where u_i represents the change in internal energy of the system, ds represents the change in entropy, dw is the mechanical work done on the system, T is the absolute temperature. The quantity Tds is the heat evolved into the system during process. It is this heat evolution that results in an increase in the entropy of the system, i.e.,

$$ds = (j \cdot E / T) dv (2.9)$$

Thus, the energy transfer from the external electric power source and the heat dissipation (q) play important roles in the microstructure transition of the ER fluid. In order to look into this phenomenon in greater detail, we shall develop a microstructure-based model for calculating the Joule heat in the suspension.

Equations for the Electric Field

Consider a dielectric sphere with a permittivity of ε_p surrounded by a fluid with permittivity of ε_f . If we apply an external field of E on this system and we take the origin of spherical polar coordinates at the center of the sphere, and the direction of E as the axis from which the polar angle is measured, then we can expect the field potential outside the sphere in the form of

$$\phi_f = -\mathbf{E} \cdot \mathbf{r} + A \, \mathbf{E} \cdot \mathbf{r} / r 3 \tag{2.10}$$

In terms of scalar quantities of r and E and the angle between r and E, which is defined by γ , we have

$$\phi_f = -Er\cos\gamma + \frac{AE}{r^2}\cos\gamma \tag{2.11}$$

The first term is the potential of the external field imposed; and the second term, which vanishes at infinity, gives the required change in potential due to the sphere. Inside the sphere, the field potential is in the form of

$$\phi_p = -BE \cdot r \tag{2.12}$$

This is the only function that satisfies Laplace's equation, remains finite at the center of the sphere, and depends only on the constant vector E. On the surface that separates two substances of different dielectric constant, certain boundary conditions must be satisfied. Assume the surface of separation is uniform as regards physical properties. One can then follow the equations of the electrostatic field for the individual phases

$$curl \mathbf{E} = 0 \text{ and } div \mathbf{D} = 0 \tag{2.13}$$

(where $D = \varepsilon E$ is the electric induction). This requires the continuity of the potential and continuity of the normal component of the induction, i.e.

$$\phi_f \mid_{surf} \mid = \phi_p \mid_{surf}$$

$$\varepsilon_p \mid \nabla \phi_p \cdot n \mid_{surf} = \varepsilon_f \mid \nabla \phi_f \cdot n \mid_{surf}$$
(2.14)

Then the constants A and B can be determined as follows:

$$A = a^3 \frac{\varepsilon_p - \varepsilon_f}{\varepsilon_p + 2\varepsilon_f}$$

$$B = \frac{3\varepsilon_f}{\varepsilon_p + 2\varepsilon_f}$$

$$E_{p} = \frac{3\varepsilon_{f}}{\varepsilon_{p} + 2\varepsilon_{f}} E \tag{2.15}$$

It is evident from equation (2.15) that the field inside the sphere has the direction of E and is uniform. It differs only in magnitude from the applied field E by a factor which is determined from the permittivity of the individual phases. If the dielectric constant of the particle is larger than that of the fluid, then the electric field inside the particle will be reduced.

In scalar format, the field outside the particle is determined from

$$E_{f,r} = -\frac{\partial \phi_f}{\partial r} = E(1 + \frac{2a^3 \beta}{r^3})\cos\gamma$$

$$E_{f,\gamma} = -\frac{\partial \phi_f}{r \partial \gamma} = -E(1 - \frac{a^3 \beta}{r^3})\sin\gamma$$
(2.16)

where
$$\beta = \frac{\varepsilon_p - \varepsilon_f}{\varepsilon_p + 2\varepsilon_f}$$
 is the dielectric mismatch parameter.

These equations for electric field of the system are consistent with those of Khusid and Acrivos (1995). The thermal properties will be incorporated with these results in the next section.

Temperature Field Resulted from Joule Heat of a Single Sphere

From experimental observation, it is found that for the pure ER liquid when exposed to strong electric field, there is almost no temperature increase. This indicates that no apparent Joule heat is created by the liquid. For an ER fluid system with considerable particle concentration, a considerable amount of Joule heating is created. In order to further understand how the existence of a large number of particles affects the ER fluid system from a thermal aspect, it is important to see how the Joule heat created by one particle influences the ER fluid system.

Consider the same system of one dielectric particle in the ER fluid as for the electric field analysis. The thermal disturbance of the particle can then be investigated from a microscopic point of view. A clue to solving this problem is based on the fact that the electric conductivity of the particles is orders of magnitude larger than that for the silicone oil (Conrad and Chen 1995); and if the particles are not sufficient in number to influence the electrical properties of the liquid, then it is found that the Joule heating is primarily created by this particle. Then the following energy equilibrium equations can be acquired:

$$div \ \lambda_p \cdot grad \ T_p + j_p \cdot E_p = 0$$

$$div \ \lambda_f \cdot grad \ T_f = 0 \tag{2.17}$$

These equations are subject to the continuous boundary conditions

$$T_p \mid_{surf} = T_f \mid_{surf} = 0; \lambda_p \nabla T_p \cdot n \mid_{surf} = \lambda_f \nabla T_f \cdot n \mid_{surf}$$
 (2.18)

where n is a unit vector normal to the surface.

Also, from the analysis of the electric field, the heating term within the particle is uniform due to the uniform electric field. Because of the geometrical symmetry of the sphere and the fact that temperature is a scalar quantity which is completely characterized by its magnitude; based in a spherical coordinate system, the temperature distribution caused by this Joule heat source is a function of the radius only. The same is true for the temperature field in the fluid since this temperature distribution is a result of the disturbance of the particle.

Based on the relation of $\sigma = j/E$ and upon introducing the non-dimensional temperature and other dimensionless parameters

$$\theta = \frac{T - T_{\infty}}{E^2 \sigma_p a^2 / \lambda_p} , R = \frac{r}{a}, \beta_1 = \frac{\varepsilon_p}{\varepsilon_f}, \beta_2 = \frac{\lambda_p}{\lambda_f}$$
 (2.19)

the following non-dimensional governing equations for the particle and fluid phases can be derived:

$$\nabla^2 \theta_f = 0 \tag{2.20}$$

$$\nabla^2 \theta_p + (\frac{3}{\beta_1 + 2})^2 = 0 \tag{2.21}$$

which are subject to the boundary conditions in dimensionless form

$$\theta_p \mid_{surf} = \theta_f \mid_{surf} = 0; \quad \beta_2 \nabla \theta_p \cdot n \mid_{surf} = \nabla \theta_f \cdot n \mid_{surf}$$
 (2.22)

From equations $(2.20 \sim 2.22)$, it is obvious that the imposition of an electric field makes the thermal conduction behavior more complicated and that the process is determined by several factors including the ratio of particle-to-fluid dielectric constant and thermal conductivity. Solving the energy equations $(2.20 \sim 2.21)$ yields

$$\theta_p = -\frac{1}{6} \left(\frac{3}{\beta_1 + 2}\right)^2 R^2 - \frac{B_1}{R} + B_0 \tag{2.23}$$

$$\theta_f = -\frac{C_1}{R} + C_0 \tag{2.24}$$

where C_0 , C_1 , B_0 , and B_1 are four constants to be determined. Boundary conditions at the interface as well as another two additional boundary conditions, i.e. the finite condition in the center of the sphere and the zero value condition as $R \rightarrow \infty$, are applied to determine these constants. Then finally, we have the solutions

$$\theta_p = -\frac{1}{6} \left(\frac{3}{\beta_1 + 2}\right)^2 R^2 + \frac{\beta_2}{3} \left(\frac{3}{\beta_1 + 2}\right)^2 + \frac{1}{6} \left(\frac{3}{\beta_1 + 2}\right)^2 \tag{2.25}$$

$$\theta_f = -\frac{\beta_2}{3} (\frac{3}{\beta_1 + 2})^2 \frac{1}{R} \tag{2.26}$$

It is apparent that the nondimensional temperature fields for both the particles and the fluid are functions of the ratio of particle-fluid thermal conductivity and dielectric constant. Fig. 2 shows the effect of the ratio of particle-fluid thermal conductivity on the temperature field around the particle. The value of $\beta_I = 2.5$ is chosen since it is a typical value for Zeolite / Silicone Oil suspensions. From Fig. 2 it can be seen that the larger the ratio of the particle-fluid thermal conductivity, the larger the increase of temperature in the field.

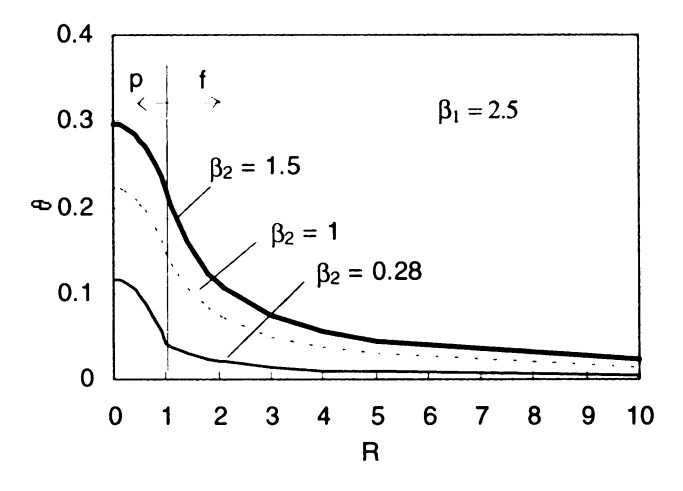


Fig. 2. Effect of Ratio of Particle-Fluid Thermal Conductivity on the Temperature Field Around a Particle

With the value of $\beta_2 = \lambda_{\text{zeolite}} / \lambda_{\text{Silicone Oil}} = 2.5$, the effect of the ratio of particle-fluid dielectric constant, β_I , is shown in Fig. 3. In contrast to the effect of the thermal

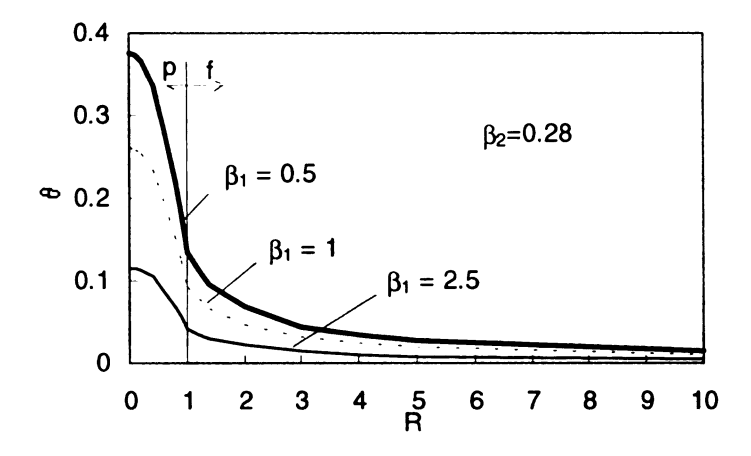


Fig. 3. Effect of the Ratio of Particle-Fluid Dielectric Constant on the Temperature Field Around a Particle

conductivity, Fig. 3 shows that the larger the ratio, the smaller is the increase in the temperature.

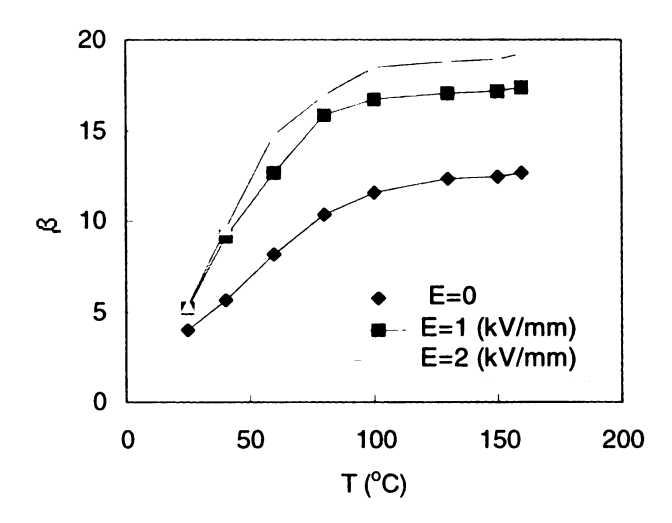


Fig. 4. Ratio of Particle-Fluid Dielectric Constant vs Temperature (Data from Conrad et al. 1991)

The response of the dielectric constant of the particles and that of the fluid to the temperature can be found in the work of Conrad et al. (1991). From the data they provided, the behavior of β_l is shown in Fig. 4. The dielectric constant of the particles increases with the temperature. The dielectric constant of the silicone oil is not thermally activated, it only decreases slightly with increasing temperature. This can explain the ER fluid design recommendation of stable electric constant for the liquid phase: As temperature increases, β_l will increase, which will suppress the further increase of the temperature (see Fig. 3). These two factors compete against each other during the development of the ordered structure.

From the above calculation, a variation in the temperature field in the suspension system is found because the electric field is able to penetrate into the particle and change the thermodynamic properties. On the other hand for a good conductor, there is no electric field inside it; and any change in its thermodynamic properties (such as entropy) amounts simply to an increase in its total energy by the energy of the field that it produces in the surrounding space. This quantity is quite independent of the thermodynamic state (and, in particular, of temperature) of the body (Landau et al. 1984), and so it does not affect the entropy and thus the order of the structure. This may explain why good conductors (or poor conductors) when dispersed do not induce any measurable ER effect. There are some reports of metal particle systems being ER active, but the strengths of the effect are quite low (Filisko 1995).

3 EXPERIMENTAL APPARATUS AND TECHNIQUE

HOMOGENOUS ER FLUIDS

Experimental Apparatus

The experimental setup for measuring thermal conductivity of the ER fluids is shown in Fig. 5. The apparatus consisted of several layers symmetrically positioned on both sides of an electric heater. In the center of the assembly is a Kapton resistance heater made of a layer of etched copper between two very thin layers of electrical insulation material. The thin layers (L= 1.6 mm) of ER fluids were vertically confined between two stainless steel plates by using a Teflon spacer. Two thermocouples whose beads were electrically insulated by poly vinyl chloride (PVC) electrically resistant tapes were imbedded into two sides of the stainless steel plates as shown. A Hewlett Packard DC

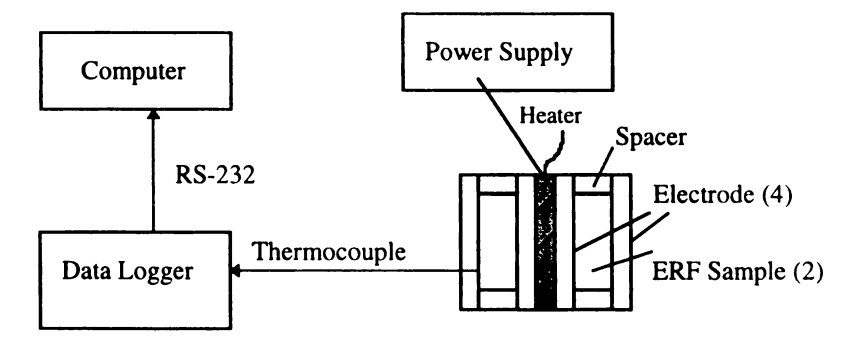


Fig. 5. Experimental Setup to Measure the Thermal Conductivity of Isotropic ER Fluid

power supply (HP model 2625) was used to provide a constant heat flux to the ER fluid samples. A Hydra Fluke 2065 data acquisition system was connected to a 486 computer through an RS-232 interface and was used to monitor and record the transient temperature data from the thermocouples. The sides of the assembly were insulated as much as possible in order to minimize the heat loss through the side normal to the heat flux plane.

ER Materials and Their Properties

A knowledge of the composition of such fluids and the properties of each individual phase is essential for any analysis of the associated heat transfer phenomena. Generally, the ER material is composed of three parts: a dispersion phase, a dispersed phase, and additives including surfactants and fluidizers (see table 4 for list of ER materials).

The dispersion could be selected from any insulating or polarized liquid, such as mineral oil or lubricant, especially silicone oil, transformer oil, cable oil, or machinery oil. The liquid should be non-conducting, non-aqueous, and have low and stable dielectric constant.

The dispersed phase may be chosen from silica gel, cellulose, and especially aluminosilicate. The size varies from 10 nm to 200µm. Typically, ER fluids consist of fine particles that have high a dielectric constant or conductivity.

The ER fluids employed in the present experiment were made of crystalline zeolite particles (UNION CARBIDE) suspended in phenmymethyl polysiloxane silicone oil (DOW CORNING). The viscosity and the thermal conductivity of the silicone oil is

0.0953 Pa-s and 0.14 W/mK, respectively. The information provided by the supplier indicates that the chemical composition of the zeolite particles is $Na_{12}[(Al_2O_3)_{12}(SiO_2)_{12}]xH_2O \text{ with a maximum of 25 wt.\% } H_2O. \text{ The main factors}$ contributing to the overall ER effect are the concentration and mobility of the charge carriers within the particles.

An ER fluid is prepared by first estimating the water content of the particles. This is done by heating the as-received zeolite particles at a temperature of 500°F for two hours (which is proved long enough to dry out all of the water) and then weighing the dry particles quickly. The dry particles are put into a steam chamber for several minutes, and the wet particles are weighed again. After the water content is thus estimated, the particles are mixed with the silicone oil to make the ER fluid with a desired particle concentration. The suspension is then stirred by a magnetic stirrer for approximately one half hour to make a well-mixed ER fluid.

Experimental Procedure

Using the parameter estimation method, two properties (λ and ρC_p) can be obtained simultaneously from a single experiment based on the governing equation

$$\frac{\partial T}{\partial t} = \alpha \frac{\partial^2 T}{\partial z^2} \tag{3.1}$$

with initial and boundary conditions

$$T^{+}(Z^{+},0) = 0$$

$$-\frac{\partial T^{+}(0,t^{+})}{\partial Z^{+}} = 1$$

$$\frac{\partial T^{+}(1,t^{+})}{\partial Z^{+}} = 0$$
(3.2)

The non-dimensional transient temperature is given by (Carslaw and Jaeger 1959)

$$T^{+} = t^{+} + \frac{1}{3} - Z^{+} + \frac{1}{2} (Z^{+})^{2} - \frac{2}{\pi^{2}} \sum_{n=1}^{\infty} \frac{1}{n^{2}} e^{-n^{2} \pi^{2} t^{+}} \cos(n\pi Z^{+})$$
 (3.3)

where

$$T^{+} = \frac{T - T_0}{qL/\lambda}, t^{+} = \frac{c\alpha t}{L^2}, Z^{+} = \frac{z}{L}$$

From the above, the non-dimensional sensitivity coefficients $X_{1,2}^+$ can be obtained. From these data we can estimate the approximate magnitude of $\Delta\lambda\sim\Delta T$ before performing the real experiment

$$X_{1.2}^{+} = \lambda \frac{dT}{d\lambda} \frac{\lambda}{aL} \tag{3.4}$$

Here, subscript 1, 2 denotes z = 0, L, respectively. It was found (Beck and Arnold 1977) that as t^+ exceeds 1, X_1^+ , and X_2^+ asymptotically approach -0.333 and 0.167. This finding helps us to determine the necessary heating time to satisfy the t^+ =1 condition and hence the maximum $X_{1,2}^+$. For our experiment, $\alpha = 3.6 \times 10^{-8}$ m²/s, L = 1.6 mm, then t = 70 sec. Therefore, we set t = 110 sec. in every measurement. The difficulties involved in property estimation for low conductivity materials such as liquids are shown through equation (3.4). Small errors found in temperature measurement could easily distort the measured value of the thermal conductivity, λ . Special effort must be made to minimize the temperature measurement errors in the experiments.

A parameter estimation program PROP1D (Beck 1989) was employed to deduce the thermal conductivity and volumetric specific heat. Parameter estimation minimizes a least square error function, s, with respect to the parameters to be estimated.

Mathematically, this involves the minimization of

$$s = \left[T_{mea} - T_{cal}\left(\varGamma\right)\right]^{tran} \left[T_{mea} - T_{cal}\left(\varGamma\right)\right]$$

where the subscript mea denotes measured data and cal denotes calculated values computed from a one-dimensional heat conduction equation with prescribed boundary conditions and an estimated property value vector. The subscript tran denotes the transposed matrix. The true value of Γ was obtained through an iteration process. An arbitrary initial value was assumed for Γ , and its value was updated at each of the subsequent iterations until convergence was obtained.

CHAIN STRUCTURED ER FLUIDS

Transient Technique

Traditionally, the thermal conductivity has been measured by the previously described transient technique with the experimental setup shown in Fig. 6.

After filling the assembly with the ER fluid, the ER fluid is left for 30 minutes to eliminate the air bubbles residing in the fluid. An electric field is then applied across the ER sample. If the current flowing through the ER fluid is low and has leveled off, the heater in the center of the experimental assembly is turned on; and simultaneously, the temperature is recorded as a function of time. After 70 seconds, the heater is turned off, and the temperature is still recorded for another 40 seconds. The thermal conductivity of the chained ER fluid is determined by calculating the input heat flux and by using PROP1D. This method has been used by Zhang and Lloyd (1993), and by Elliott (1997).

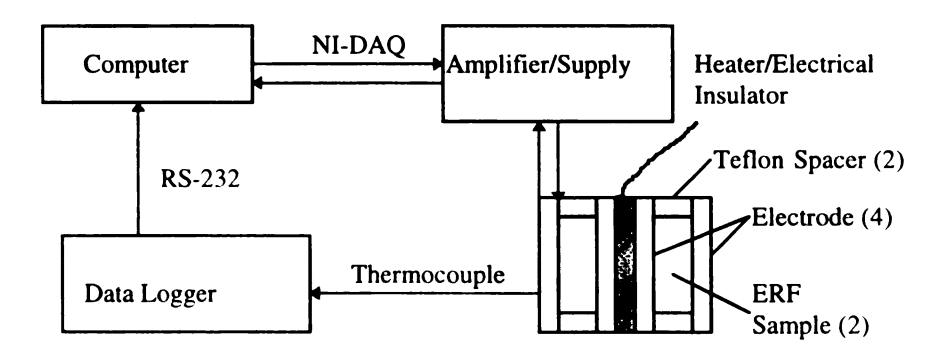


Fig. 6. Experimental Setup to Measure the Thermal Conductivity of ER Fluid with Electric Field

Internal Heat Generation Technique

Theoretical Background. As the electric current passes through the ER sample, the ER fluids rise in temperature and dissipate heat. When the ER fluids are exposed to high electric fields and if significant current flows through the fluid, there exists a heat source within the volume of the sample. From the open literature and from our experimental observations, it is found that for a given electric field, the current density increases with time at the first stage of the experiment, and then as time moves on it levels off indicating the heat source in the ER fluid or the fluid state remains constant. When the system reaches a steady state, the thermal conductivity of the chained structure ER fluid can be determined. This is illustrated in more detail as follows.

The experimental setup for this volume heat source technique is the same as the one shown in Fig. 6. Here, the heater in the center of the assembly has been replaced by an electrical insulator. The Joule heat generated in the ER fluid is used as the heat source to measure the thermal conductivity, and it is obtained by measuring the current density and the applied voltage. In order to satisfy the one-dimensional conduction condition, a value of 21 is chosen for the ratio of the diameter of the electrode to the distance between the two electrodes. The round sides of the assembly have been insulated as much as possible to minimize the side heat loss. The ER sample has an insulated boundary condition on one side and a natural convection condition on the other side, which will ensure the one-dimensional conduction process.

At the first glance at the energy equilibrium equation, it seems hard to measure λ without measuring the temperature distribution within the ER sample to get the value of

 $\lambda = \frac{j \cdot E}{\partial^2 T / \partial^2 z}$. However, solving equation (3.5) with the appropriate boundary conditions makes this possible.

$$\lambda \frac{\partial^2 T}{\partial^2 z} + j \cdot E = 0 \tag{3.5}$$

If we assume that at steady state, the thermal conductivity, λ is a constant, we can obtain the temperature field as follows:

$$T = -\frac{jE}{2\lambda}z^2 + a_1z + a_0 \tag{3.6}$$

From the design of the experiment, at z = 0, an insulated boundary is imposed, which makes a_I equal to zero. The unknowns λ and a_0 can then be determined by measuring the temperatures at the boundaries of z = 0 and z = L, denoted as T_{0i} and T_{li} respectively. Thermal conductivity, λ , can then be evaluated from the equation:

$$\lambda = \frac{jEL^2}{2(T_{0i} - T_{Li})} \tag{3.7}$$

In the present experiment, due to the application of the high electric field, and because of the requirement to electrically insulate the thermocouple from the fluid, the

thermocouple is embedded on the outer surface of the electrode. Therefore, the quantity measured is T_0 and T_L (though $T_0 = T_{0i}$ in our case). This is illustrated as follows in Fig. 7 by considering half geometry of the ER assembly. A correction for the evaluation is made as follows in order to minimize the error associated with the model.

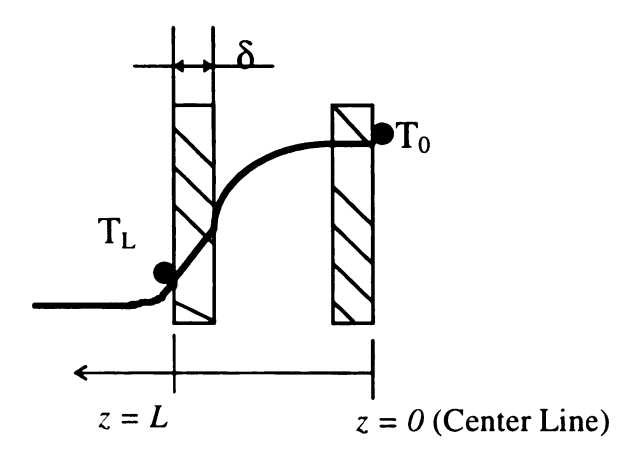


Fig. 7. Schematic of Temperature Field in Half of the Symmetry ER Assembly

Here

$$\lambda = \frac{(jE)_{st} L^2}{2((T_0 - T_L)_{st} - \frac{(jE)_{st} \delta}{\lambda_{steel}})}$$
(3.8)

where the subscript st refers to the value at steady state, and δ and λ_{steel} refer to the thickness and thermal conductivity of the stainless steel electrode. The thermal resistances for the components used in the composite specimen of the assembly are listed

in Table 1. It can be seen that compared to that of the ER fluid sample the thermal resistance of the stainless steel is negligible.

Table 1. Characteristics of Components of the Composite Specimen

	Thickness,	Thermal	Thermal Resistance, δ/λ
	δ(mm)	Conductivity, λ	$(10^{-4} \text{ m}^2\text{K/W})$
		(W/mK)	
Stainless Steel	0.45	14.7	0.3
ER Fluid	1.6	0.16±0.01	106.3

Experimental Procedure. A LabVIEW VI program has been written up for the data acquisition and processing in the measurement. The control of the applied voltage and the data recording of the current and voltage are realized by sending commands in the LabVIEW VI program and through the NI-DAQ interface.

An ER fluid is prepared in the same way described in the previous two sections. About 30 minutes after the assembly is filled with the well-mixed ER fluid, an electric field is applied across the ER sample. By using the LabView program the temperature, the voltage across the ER fluid layer, and the current flowing through the ER fluid were recorded simultaneously as functions of time.

When the current as well as the temperature (or temperature difference) levels off, it is assumed that the system has reached its steady state. The Joule heat is calculated from the product of the electric field and the current density at steady state based on equation (2.7). The thermal conductivity is determined based on equation (3.8). This

procedure is repeated for the fluids with several particle concentration and at different levels of electric field.

4 RESULTS AND DISCUSSION

SILICONE OIL AND ZEOLITE PARTICLE CALIBRATIONS

To confirm the reliability of the experimental system, the thermal conductivity of the silicone oil was measured by both transient and steady state methods. Transient methods allow faster determination of the thermal conductivity. The value is obtained from the rate of the establishment of the thermal gradient in the suspending medium system. While, in steady state methods, the value is determined from the final thermal

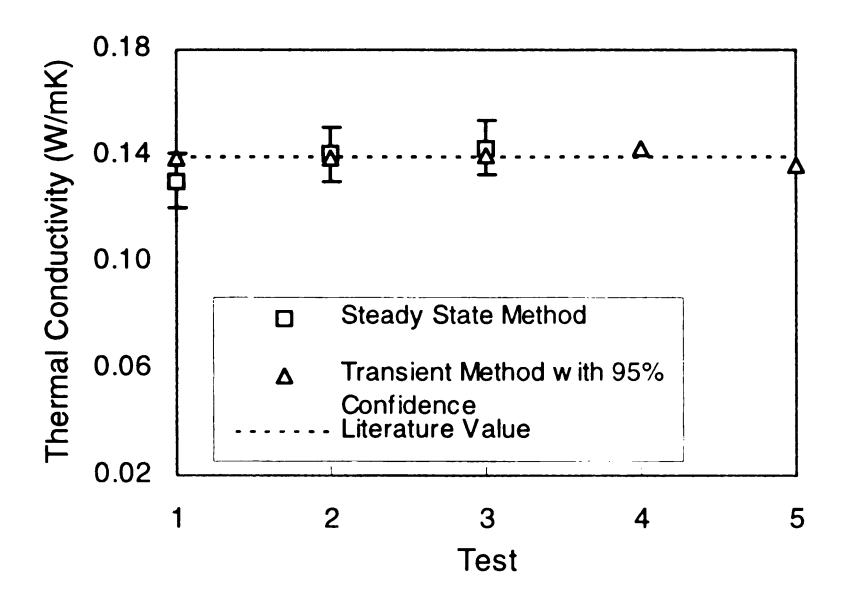


Fig. 8. Thermal Conductivity of Silicone Oil

gradient which takes about four hours to establish. Both of the experiments were conducted with the same heat flux of 478 W/m².

Fig. 8 shows the results from several experiments. It is shown that the discrepancy between the results from PROP1D and those from steady state are negligible. The measurements exhibit very good repeatability. Furthermore, the value is close to that given by the supplier (0.14 W/mK).

Zeolite particles exist in the form of a powder. In order to measure its thermal conductivity the first step is to put the zeolite powder into the test assembly. After packing the powder as much as possible the zeolite in the assembly looks like a solid. The assembly is then closed for the measurement process. The rest of the procedure for the measurement is very similar to the measurement of the thermal conductivity of the silicone oil and is done by transient method and determined by PROP1D. The value comes out to be 0.039 W/mK which is very close to the literature value, 0.04 W/mK.

HOMOGENOUS ER FLUIDS

Comparison Between Prediction and Measurement

The thermal conductivity of the ER fluids with zero electric field was measured using the transient method. The results are shown in Fig. 9. It shows some discrepancies between the calculated values from equations (2.1) and (2.5) and the measured values, while the discrepancies between prediction from equation (2.4) and the measured value are smaller. Interestingly, the prediction of equation (2.1) and that of equation (2.5)

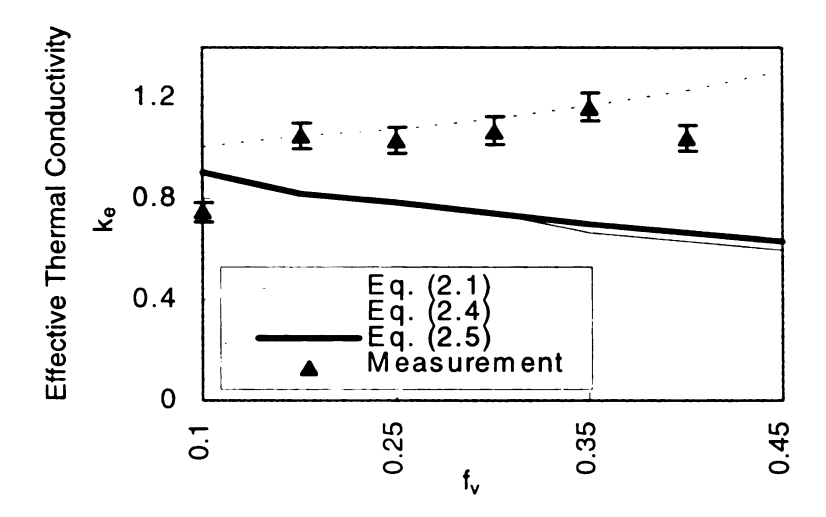


Fig. 9. Thermal Conductivity of Zeolite/Silicone Oil Suspension

happens to be almost the same. It is of pragmatic importance to study the possible reasons behind these discrepancies and coincidences.

From the agreement between the prediction of equation (2.4) and the measurement and from the fact that equation (2.4) is based on the assumption of linear heat flow in the fluid, we can infer that the heat flow in the ER suspension with no electric field is linear. The model from the statistical method and the model that accounts for only dipoles and octupoles under-estimate the thermal conductivity of the isotropic ER fluid at the same scale. Obviously higher orders of interaction between the particles must be considered for the isotropic ER fluid.

One of the possible reasons for the relatively high thermal conductivity of the ER fluid is the special structure of zeolite particles as described previously. For pure particles, the open channels of the framework are filled with air, which has a thermal conductivity of only 0.026 W/mK. Actually, the air makes a large contribution to the low

thermal conductivity of the zeolite crystal (0.04 W/mK). When dispersed in the silicone oil, the channels are occupied by the oil whose thermal conductivity is 0.14 W/mK. Besides, when the suspension becomes dense, the particles come into close contact; and the intermolecular forces will increase to an extent which will draw the particles together into tighter contact and this will result in higher thermal conductivity.

34

Another obvious reason is the existence of water in the solution. The addition of this third component can cause considerable change to the properties. The thermal conductivity of water is about 0.59 W/mK, which is much larger than that of the zeolite and of the silicone oil. Little information can be found to theoretically predict the effective thermal conductivity for such a three-component system. As a qualitative analysis, assume H₂O wt.5% in the solution, then the effective thermal conductivity is

$$\lambda_e = 0.05 \times 0.59 + 0.95 \times 0.14 = 0.16 \text{ (W/mK)}$$

which indicates that the existence of water can result in a higher thermal conductivity of the wet fluid.

Temperature Effect

Changes in temperature due to electrical power dissipation in the fluid may significantly change the properties of an ER fluid. Understanding the temperature effect on ER properties is critical to further predict the ER behavior.

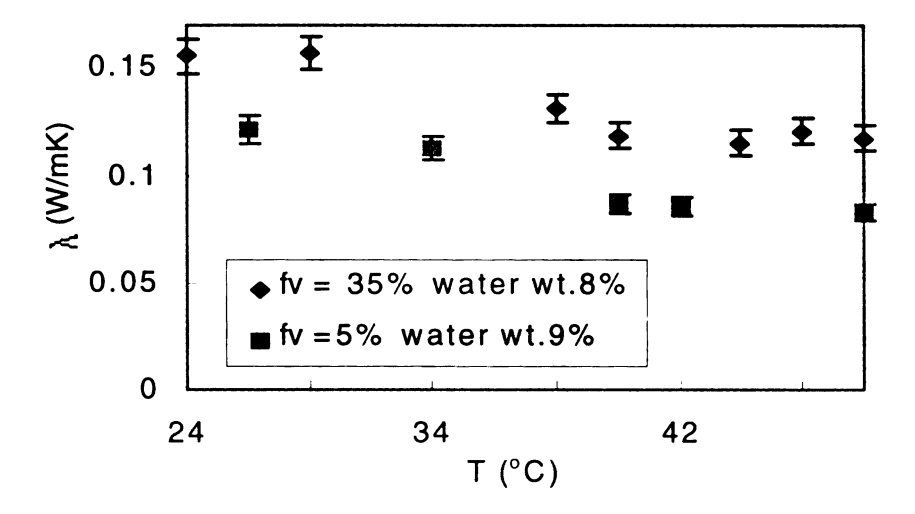


Fig. 10. Temperature Effect on the Thermal Conductivity, λ of Isotropic ER Fluid

The temperature dependence of the thermal conductivity of a uniformly dispersed ER fluid over the range of 24°C - 50°C is shown in Fig. 10. It shows that the thermal conductivity decreases slightly as the temperature increases. This phenomenon is similar to the viscosity property, which decreases as the temperature increases, and it indicates that the fluid is temperature "thinning" (Nelson and Suydam 1993). When the temperature increased from 24°C to 50°C , the thermal conductivity decreased from 0.13 W/mK to about 0.08 W/mK for fluids with $f_v = 0.05$, and from 0.15 W/mK to 0.10 W/mK for fluid with $f_v = 0.35$.

This result contrasts with the response of the electrical conductivity and dielectric constant (Conrad et al. 1991, Conrad and Chen 1995) and is unexpected. If the electrical conductivity and dielectric constant changes as a result of the diffusion of Na⁺ ions in the zeolite particles and the mobile charge carriers whose number or mobility are thermally activated, then a higher thermal conductivity should be expected since there are more

energy carriers at higher temperature. But the result suggests that prior to the application of an electric field the isotropic ER fluid behaves like a "regular" liquid, i.e. the viscosity as well as the thermal conductivity of the fluid decreases with increasing temperature. Though the fluid contains ions and charge carriers, the thermal conductivity is still different from the system with charged-particles, such as liquid metals with abnormally high thermal conductivity. In liquid metals, according to Wiedemann-Franz-Lorenz law, the value of $\mathcal{N}\sigma T$ is almost a constant, which indicates that the current carriers are electrons and that the current carriers must also be important in heat conduction (Tye 1969). In a word, for the isotropic ER fluid, the roles of the ions and other charge carriers are not dominant in the heat conduction process.

CHAIN STRUCTURED ER FLUIDS

Results from Transient Technique

Part of the data obtained by the transient technique is shown in Table 2. It demonstrates a 37% increase in thermal conductivity with application of an electric field.

Zhang and Lloyd (1993) using a similar ER fluid found a 55% increase. In the application

Table 2. Thermal Conductivity, λ , of ER Fluid as a Function of Applied Electric Field ($f_v = 35\% H_2O \text{ wt.}8\%$)

E (V/mm)	Average	λ (W/mK)	
	Temperature (°C)		
0	25	0.16±0.01	
500	35	0.19±0.01	
1000	35	0.22±0.01	

of transient technique, the thermal conductivity is determined from the transient temperature gradient and the heat flux supplied by the heater. The Joule heat, which composes of part of the heat flux being conducted out, has been omitted. Therefore, the transient method has under-predicted the thermal conductivity of the chained ER fluids.

Results from Internal Heat Generation Technique

ER Phenomenon. Traditionally, the ER effect was reflected by the electric current density. For our study, when an electric field was applied to the ER fluid, three types of current profiles (versus time) were found, as shown in Figs.11-13. With a low electric field, the current density increases exponentially to reach a constant (Fig.11), or increase exponentially to reach a peak value then slightly drops down to reach a constant (Fig.12). The temperature increase in the fluid caused by Joule heat is small (usually less

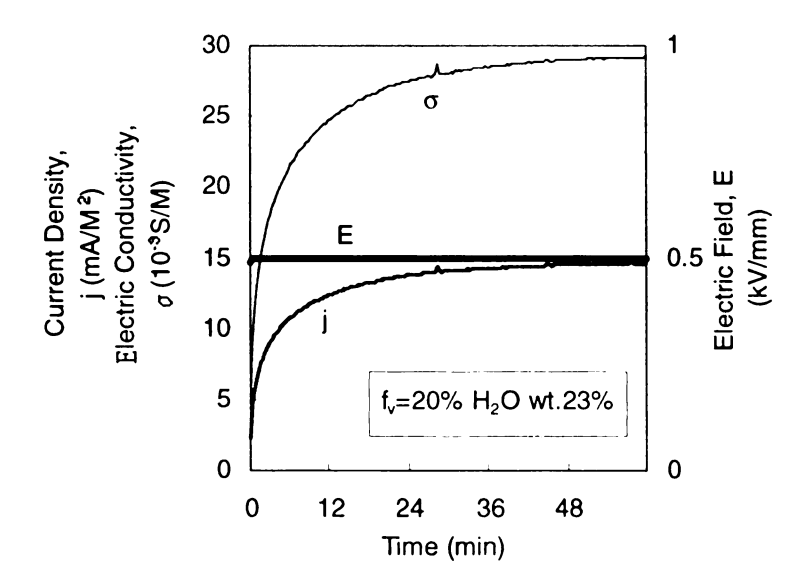


Fig.11. Electric Property Response of ER Fluid with Low Electric Field and High Water Content

than 10°C), which is far below the boiling point of water. These two types of response are basically stable since the water content remains approximately constant.

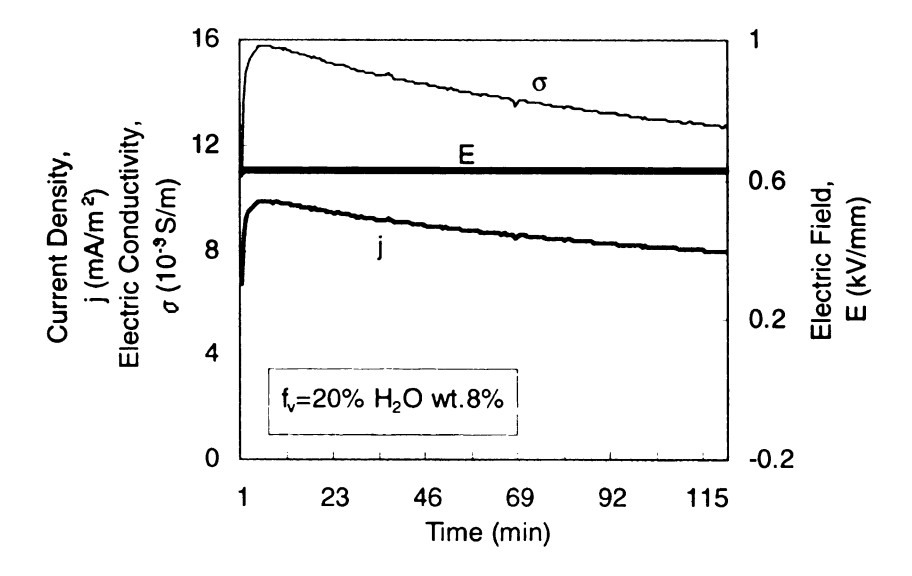


Fig. 12. Electric Property Response of ER Fluid with Low Electric Field and Low Water Content

When the electric field is high (in Fig. 13, E = 0.75 kV/mm), the current density shoots up sharply at the first stage of the experiment and reaches the current limit of the amplifier (here 5.0 mA). In the meanwhile, a large amount of heat is created within the fluid, which causes pronounced temperature increase (from 23°C to 84°C after 46 minutes of heating, see Fig. 14). This result strongly depends on the water content.

From this experimental observation and the analysis in chapter 2, we can see that at first, the ER effect is caused by the application of the external field. As long as the Joule heat is created and the ER fluid is subject to a thermal disturbance, the thermal properties and electric properties of the ER material, and the water content will vary if the

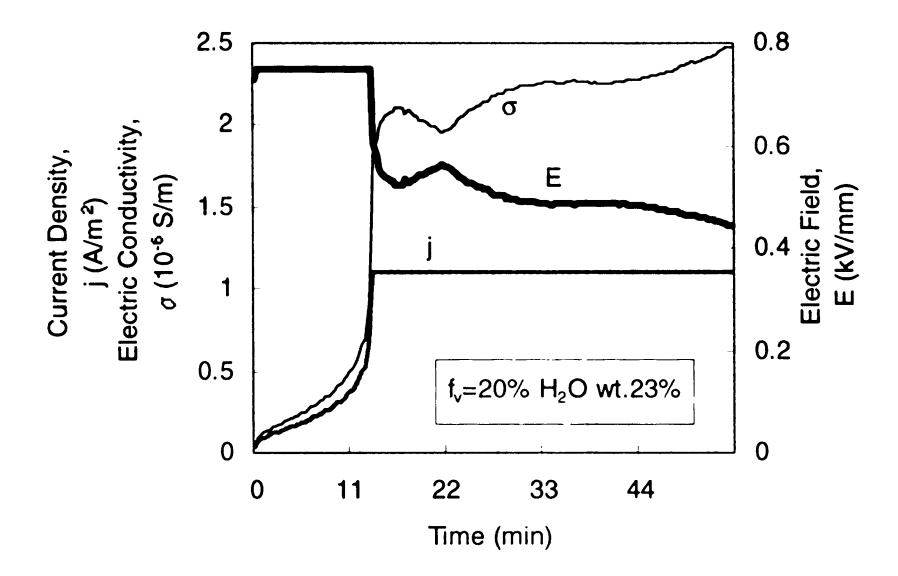


Fig. 13. Electric Property Response of ER Fluid with High Electric Field and High Water Content

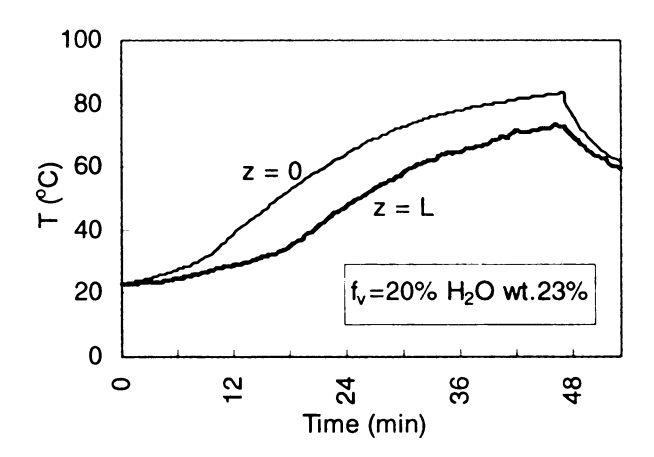


Fig. 14. Typical Temperature Profile of ER Fluid Exposed to Electric Field

temperature increase is considerable, which in turn will influence the local electric field of the ER system as well as the strength of the chaining. As the ER effect varies, the temperature field begins to change, and a new cycle of the adjustment of all of the parameters will start again. The cycle will continue until all of these mutual effects have

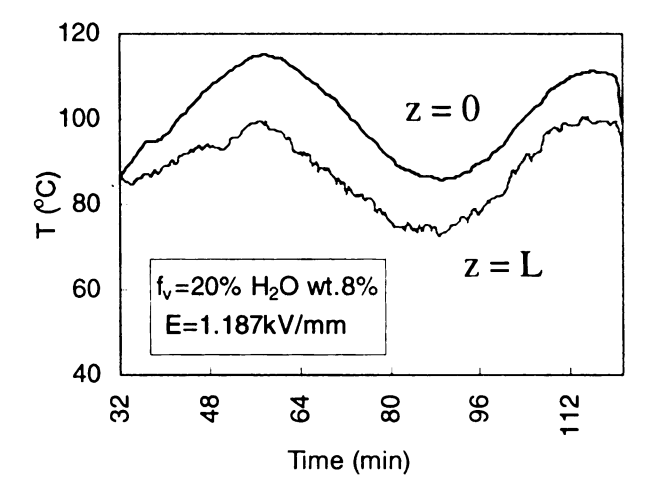


Fig. 15. Temperature Fluctuation of ER Fluid

reached a compromise status where the steady state is reached. If the competition between these parameters are comparable, it may result in a slow sine-wave like temperature fluctuation as was measured and is shown in Fig. 15. Typically, it takes three hours for the Zeolite/Silicone Oil ER fluid to reach steady state.

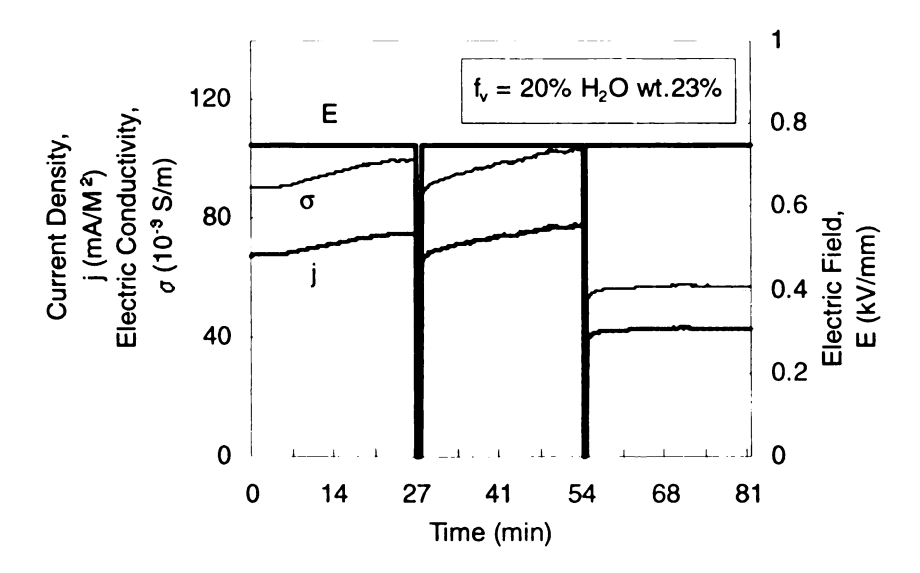


Fig. 16. Dependence of the ER Effect on the Initial States

The effect of the ER fluid strongly depends on the initial state of the fluid. This fact is demonstrated by turning the electric field off for a minute and then turning on again. The effect of the initial structure on the current density of the ER fluid is shown in Fig. 16. It shows that when a same E is applied to the ER fluid, which has exposed to the electric field previously, a lower current density results. In order to make the results comparable, initial conditions for the measurement should be taken into account for all of the measurement of the thermal conductivity of the ER fluid.

It can provide a useful insight into the ER phenomenon to look back to the work of Adrian and Gast (1988) where they have introduced a parameter, ζ , that expresses the ratio of polarization to thermal forces

$$\zeta = \frac{\beta^2 E^2 a}{4\varepsilon_f k_B T} \tag{4.1}$$

Here a is the radius of the particles, k_B is Boltzmann's constant. They found that electrically determined structures were likely to occur only if the electrical forces can overcome the thermal forces. Obviously, the ordered structure of the ER system is caused by the external electric field. Only in the in the limit ζ >>1 can an effective ER effect occur. Based on this model, when a temperature increases due to the application of an electric field, the polarizability must also increase in order to maintain the value of ζ to a

certain value. Only the material whose properties satisfy this condition can be applied as ER materials. This can be one of the clues for the design of ER materials.

For the case where the fluid dielectric constant, ε_f remains about constant during the process, the only variables we are interested in are $E^2\beta^2/T$. The value for the dielectric mismatch parameter, β , can be obtained from the work of Conrad et al. (1991) for this particular case (temperature shown in Fig. 14). As the temperature increases from 23°C to 84°C, $E^2\beta^2/T$ changes from around 5.7×10^{-4} to 4.1×10^{-4} , thus indicating that the ratio of the polarization force to the thermal force is decreased, and an electrically induced ER fluid chain structure may not be maintained or might break down. For this case a very low thermal conductivity ($\lambda = 0.06$ W/mK) results.

This result is in contrast with the observation by Conrad et al. (1991) where they found that the strength of the chaining of ER fluid increased with temperature. However, the present result is consistent with the work of Oyadiji (1995), in which he found that the shear modulus of the ER fluid decreased with the temperature increase from 0 to 60°C.

Thermal Conductivity. There are several factors such as water content, temperature, and ER effect that determine the thermal conductivity of an activated ER fluid. Among those parameters, the effect of temperature together with the ER effect is the dominant one. If strong chaining can be obtained at low temperature, then the ER fluid at that state has a high thermal conductivity and the result will be more repeatable. The data for the fluid of $f_v = 10\%$ with H_2O wt.19% is shown in Table 3. These data have shown a 83% increase in the thermal conductivity when an electric field of 250 V/mm is

Table 3. Thermal Conductivity, λ , of ER Fluid as a Function of Applied Electric Field ($f_v = 10\% \text{ H}_2\text{O wt.}19\%$)

E (V/mm)	J (mA/m ²)	Average	λ (W/mK)
		Temperature (°C)	
250 (run 1)	339.6	30	0.27±0.05
250 (run 2)	311.4	30	0.28±0.03
0	0	27	0.15±0.01

applied across the ER fluid and it has shown a good reproducibility. Note here the electric field is very low.

Refer to the data shown in Table 2, for example, at an electric field of 1000 V/mm, the thermal conductivity enhancement is 37% based on the transient technique without considering the Joule heat. However, for the ER fluid exposed to an electric field, in addition to the surface heat flux, q_s , supplied by the heater that has been intentionally turned on to established a transient condition, a volumetric heat created by Joule heat should be included in the heat equation

$$\rho C_p \frac{\partial T}{\partial t} = \lambda \frac{\partial^2 T}{\partial x^2} + q \tag{4.2}$$

where q is the Joule heat. For the experimental sample in the transient technique, the surface heat flux is supplied after the chaining is developed. If q is considered to be constant at the time the measurement is being taken, then q represents an initial heat

exchange and may depend on z, but is independent of time. Because of the linearity of the differential equation (4.2), q and q_s produce independent temperatures $T_J(z)$ and $T_s(t, z)$. Therefore, the initial steady-state temperature distribution $T_J(z)$ satisfies the steady-state equation of (3.5) which will be shown here again in the format as follows

$$\lambda \frac{\partial^2 T_j}{\partial x^2} + q = 0 \tag{4.3}$$

Subtracting equation (4.3) from equation (4.2), and based on the fact that $T_J(z)$ is independent of time, we have

$$\rho C_p \frac{\partial (T - T_J)}{\partial t} = \lambda \frac{\partial^2 (T - T_J)}{\partial x^2}$$
(4.4)

This indicates that the actual thermal conductivity of the chained structured ER fluid should be determined based on the transient temperature T- $T_J(z)$ if we will use transient technique. Here $T_J(z)$ is already solved in Chapter 3 and shown in Fig.7. It is possible to make some corrections to the results from the transient technique.

It is useful to utilize a specific example in Table 2, for example with application an electric field of 1000 V/mm, a thermal conductivity of 0.22 W/mK is determined based on equation (3.1) which will be shown here again in the following format

$$\rho C_p \frac{\partial T}{\partial t} = \lambda \frac{\partial^2 T}{\partial x^2} \tag{4.5}$$

Recall that the final value of the thermal conductivity was determined based on the surface heat flux q_s and from the transient temperature profiles (T in Fig. 17).

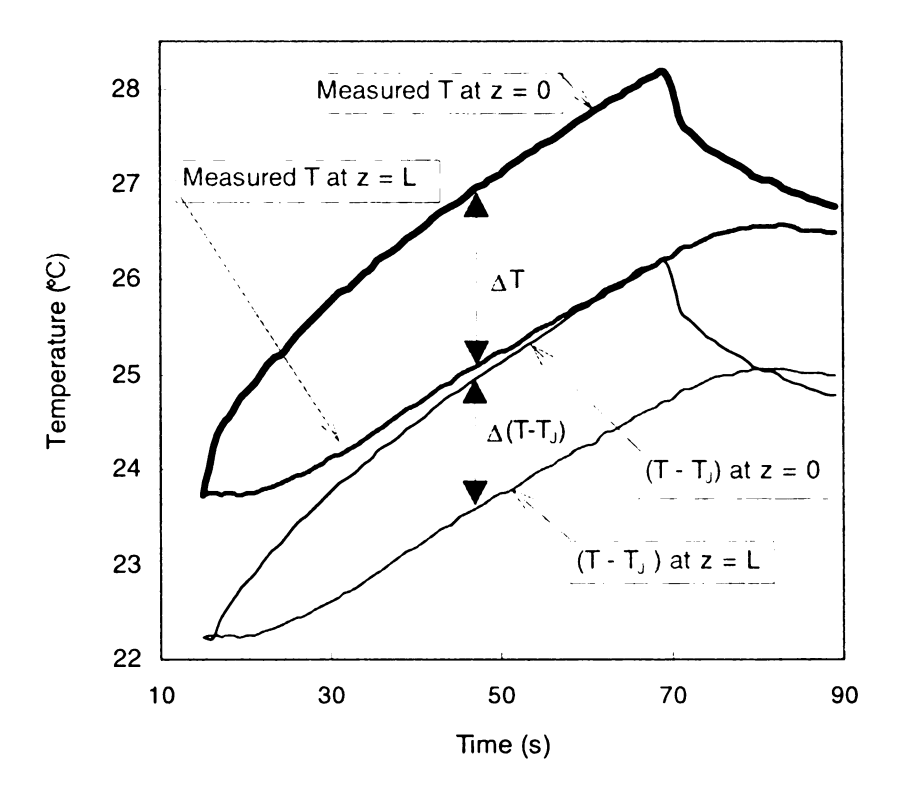


Fig. 17. Transient Temperature Profiles for T and $(T-T_J)$ at Positions of z = 0 and z = L

The transient temperature of T(t,z) - $T_J(z)$ can be obtained by subtracting the temperature value $T_J(z)$ at z=0 and z=L (denoted as $T_J(0)$ $T_J(L)$) from the measured temperatures T. Based on this corrected transient temperature gradient and using PROP1D program, the actual value of the thermal conductivity of the chained structured ER fluid can be estimated. It is obvious that $T_J(0) > T_J(L)$ (Fig. 7). and these values are

independent of time. In the transient technique, the results are very sensitive to the value of temperature difference between the two electrodes, ΔT , a decrease in ΔT will result in a high value of λ .. The temperature difference used in the case with consideration of Joule heat ($\Delta (T-T_J)$ in Fig. 17) is smaller than that in the case without consideration of Joule heat (ΔT in Fig. 17). Therefore with the corrected temperature profiles, a higher value of thermal conductivity is obtained.

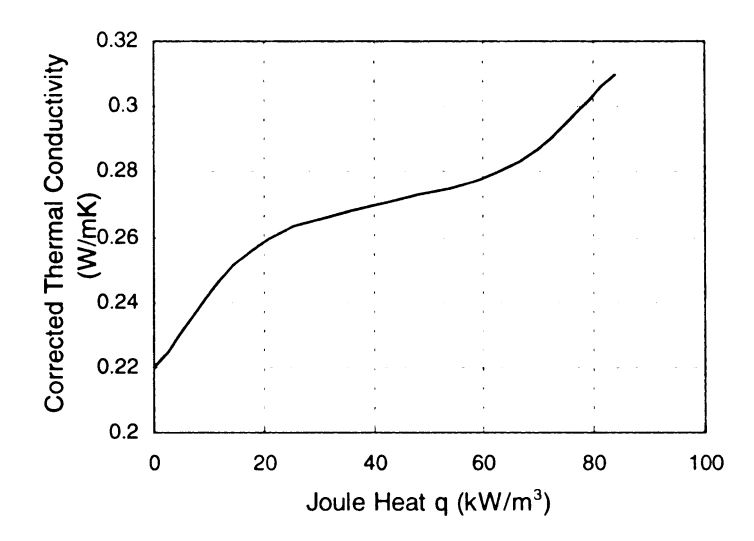


Fig. 18. A Correction to the Thermal Conductivity of the Structured ER Fluid with Consideration of Joule Heat

The calculation for consideration of several values of Joule heat in the previous case is shown in the Fig. 18. It is seen that with consideration of Joule heat, a higher value for the thermal conductivity can be obtained based on the level of the Joule heat. For example, if a Joule heat of 80 kW/m³ (estimated from Table 3) is considered, a corrected value of 0.31 W/mK can be expected, instead of a value of 0.22 W/mK which is determined by the traditional transient technique without consideration of Joule heat. A considerable error is involved due to the neglect of Joule heat.

In dependent of the measurement techniques, it requires that the data be reproducible. The data in Table 3 are repeatable because the current is low; thus, the temperature increase caused by Joule heat is under low level and the structure of the fluid is under control. In order to obtain good and reliable data, the humidity and temperature of the environment should be well controlled for ER fluid with water as an important activator.

As the temperature increases to a high value, the measurement of the thermal conductivity becomes difficult since the water in the ER fluid can evaporate off. A certain volume of ER fluid may be boiled out depends on the temperature level. This result is not repeatable without good control of the humidity and temperature of the environment. Measured results from several experiments running at high temperature show a very low thermal conductivity When the temperature is very high, the value for λ at the corresponding state is counteracted by the "thinning effect" caused by the temperature

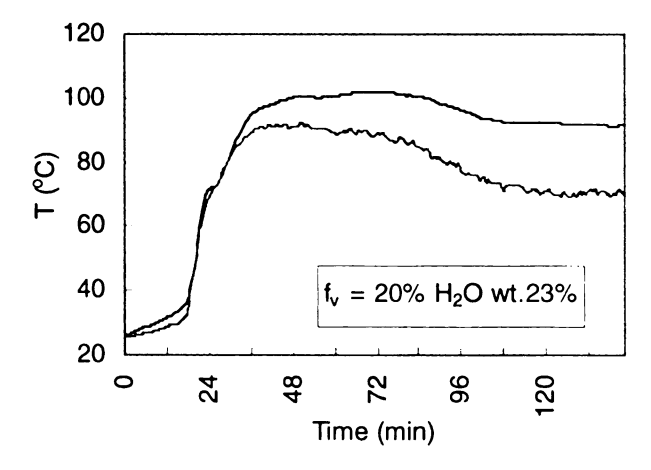


Fig. 19. Temperature Profile of ER Fluid at High Electric Field

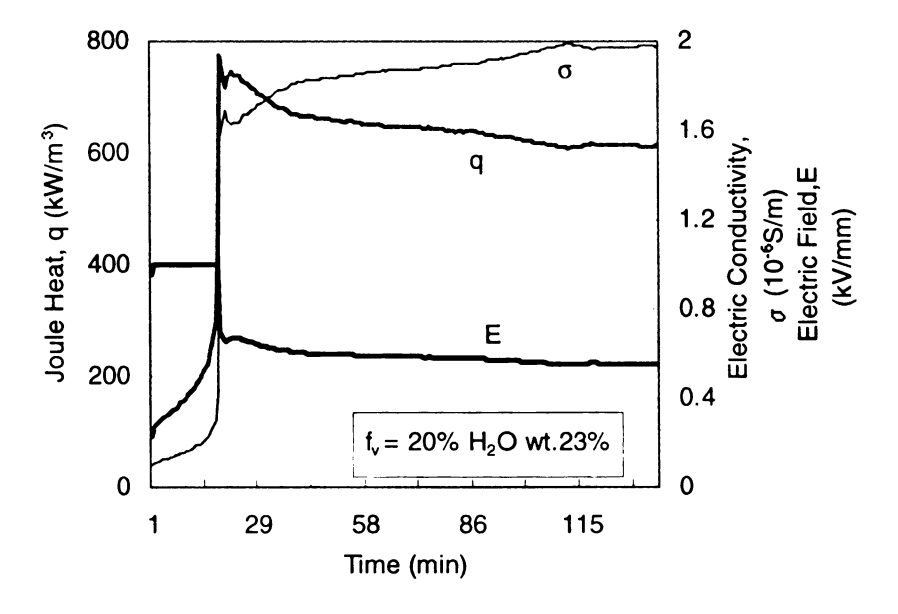


Fig. 20. Joule Heat and Electric Conductivity of ER Fluid at High Electric Field

increase therefore its value is very low. A calculation shows $\lambda = 0.039$ W/mK for the fluid of $f_v = 20\%$ H₂O wt.23% when this fluid is exposed to high electric field (see Figs. 19 ~ 20 for temperature and electrical property response).

Similar to the discovery about the diatomaceous earth / oil suspensions (Shulman, 1982), at high temperature, the ER effect decreases due to desorption of the activator from the particles to the continuous phase, the loss of water in the present Zeolite / Silicone Oil suspension also cause the decrease of ER effect. This also indicates that the current level is not the equivalent of ER effects. This is the reason for the fully chaining ER fluid, the overall thermal conduction is enhanced to a large extent depending on the micro structure states of the ER suspensions. With the ER fluid exposed to electric field, the contribution of the transport of ionization energy to thermal conduction should lead to a high value of the thermal conductivity in the ER fluid. On the other hand, as

temperature increases, the Brownian motions will prevent the energy transfer between the particles.

When a high electric field is applied upon the wet ER fluid, the temperature of the ER fluid is increased dramatically from 25°C to over 120°C. The particles alignment between the two electrodes has resulted in solid-like material, while the foam-like liquid are flowing out of the chamber, then after temperature reaches a very high level and some of the water has been boiled off, what left on the chamber is cone-like solid. Each experiment should start with clean apparatus using fresh fluid in order for the results to be comparable.

Another point which deserves to be discussed is the air bubbles in the fluid. If considerable number of air bulbs exit in the fluid, these bulbs can be a source of more bulbs when electric field is applied, which will make the thermal conductivity reduce to a very low value (0.02~0.06 W/mK). Therefore it is very important to make sure that the air is dissipated out completely before application of electric field.

From the above discussion, it can be inferred that the thermal conductivity of the chain structured ER fluid strongly depends on several factors such as water content, temperature, electric field, and ER effect. Among these, water content and temperature are the dominant factors controlling the thermal conductivity of the ER fluid exposed to an electric field. The higher the temperature, the lower the thermal conductivity; the stronger the chaining, the higher the thermal conductivity. An optimum water content should make it possible to form strong chaining at low temperature in order to enhance the heat conduction.

5 CONCLUDING REMARKS

The theoretical analysis about the temperature field caused by the Joule heat of the particles and the experimental evidence that incorporate the thermal properties and electrical properties into the ER effect have provided a good understanding of the mechanism for the development of the chaining.

Transient method has been proved to be appropriate for the measurement of the thermal conductivity of silicone oil and isotropic ER fluid. The investigation of the temperature effect on the thermal conductivity of the isotropic ER fluid has shown that as the temperature increases, the thermal conductivity of the isotropic ER fluid decreases.

A newly-proposed measurement approach - internal heat generation technique, which uses Joule heat as the power source, has been successfully used to measure the thermal conductivity of the chain structured ER fluid. It is found that water content and the temperature are the dominant factors controlling the thermal conductivity of the ER fluid exposed to an electric field. The higher the temperature, the lower the thermal conductivity. The measured results have manifested an augmentation of heat conduction (83% increase in the thermal conductivity when an electric field of 250 V/mm is applied across the ER fluid) when strong chaining is formed at a low temperature.

In order to make full use of the ER fluid which uses water as an activator, further research work is needed and should focus on the control of the water content of the ER fluid and the control of the temperature of the ER fluid during the development of the chaining.



BIBLIOGRAPHY

Adriani, P. M. and Gast, A.P., 1988, Phys. Fluids 31, 2757.

Beck, J.V. and Arnold, K.J., 1977, "Parameter Estimation in Engineering and Science", John Wiley and Sons, New York.

Beck, J.V., 1989, "PROP1D - Parameter Estimation Computer Program", Michigan State University.

Block, H. and Rattray, P., 1995, "Recent Developments in ER Fluids", *Progress in Electrorheology*, Edited by Havelka, K. O., and Filisko, F. E., Plenum Press, New York, pp.19-42.

Conrad, H. and Chen, Y., 1995, "Electrical properties and the strength of electrorheological (ER) fluids", *Progress in Electrorheology*, Edited by Havelka, K. O., and Filisko, F. E., Plenum Press, New York, pp.55-84.

Calson, J.D. and Duclos, T.G., 1989, "ER Fluid Clutches and Brakes - Fluid Property and Mechanical Design Considerations". In *Electrorheological Fluids: Proceedings of the Second International Conference on ER Fluids Held in Raleigh, North Carolina, August 7-9, 1989*, edited by J.D. Carlson, A.F. Sprecher and H.Conrad, Lancaster: Technomic Publishing Co., pp. 353-367.

Conrad, H., Sprecher, A. F., Choi, Y., and Chen Y., 1991, "The temperature dependence of the electrical properties and strength of electrorheological fluids", J. Rheol Vol.35, No.7, pp.1393-1410.

Coulter, J.P. and Duclos, T.G., 1990, "Applications of Electrorheological Materials in Vibration Control". In *Electrorheological Fluids: Proceedings of the Second International Conference on ER Fluids Held in Raleigh, North Carolina, August 7-9, 1989*, edited by J. D. Carlson, A. F. Sprecher and H. Conrad, Lancaster: Technomic Publishing Co., pp. 300-325.

Davis, L. C., 1992, "Polarization forces and conductivity effects in electrotheological fluids", J. Appl. Phys., Vol. 72, No. 4, pp.1334-1340.

Dukhin, S. S. and Shilov, V. N., 1974, "Dielectric Phenomena and the Double Layer in Disperse Systems and Polyelectrolytes" (Wiley, New York).

Elliott G. D., 1997, "An Investigation of The Potential For Controllable Heat Transfer in Electrorheological Fluid Composites", Master's Thesis, Michigan State University, East Lansing, Michigan.

Filisko, F. E., 1995, "Overview of ER Technology", *Progress in Electrorheology*, Edited by Havelka, K. O., and Filisko, F. E., Plenum Press, New York, pp.3-18.

Gast, A. P. and Zukoski, C. F., 1989, "Electrorheological Fluids as Colloidal Suspensions", Adv. Colloid Interface Science, Vol. 30, pp. 153. Hartsock, D. L., Novak, R. F., and Chaundy, G. J., 1991, "ER Fluid Requirement for Automotive Devices", Journal of Rheology 35, pp. 1305-1326.

Hamilton, R. L., and Crosser D. K., 1963, "Thermal Conductivity of Heterogeneous Two-component Systems", Ind. Engng. Chem. Fundamentals 1, pp. 187-197.

Khusid, B., and Acrivos A., 1995, "Effects of conductivity in electric-field-induced aggregation in electrorheological fluids", Phys. Rev. E, Vol. 52, No. 2, pp.1669-1693.

Klass, D. L. and Martinek, T. W., 1967a, "Electroviscous fluids I: Rheological properties", J. Appl. Phys. 38(1), pp. 67-74.

Klass, D. L. and Martinek, T. W., 1967b, "Electroviscous fluids II: Electrical properties", J. Appl. Phys. 38(1), pp. 75-80.

Korobko, E. V, 1992, "The Main Properties of ERF's and Their Application", Conference on Recent Advances in Adaptive and Sensory Materials and Their Applications, Blackburg, Virginia.

Landau, L. D., Lifshitz, L. P. and Pitaevski, L. P., 1984, *Electrodynamics of Continuous Media*, Pergamon, Oxford.

Li, J., Jin, D., Zhang, X., Zhang, J., and Gruver, W. A., 1995, "Electrorheological Fluid Damper for Robots", Proceedings - IEEE International Conference on Robotics and Automation, Vol. 3, pp. 2631-2636.

McGregor, K.R., 1997, "Precise Control of Electrorheological Fluids in Composite Structures", Master's Thesis, Michigan State University, East Lansing, Michigan.

McLaughlin, E., Trans. Faraday Soc., 55, 21.

Morishita, S., An, Y. K., and Mitsui, J., 1995, "ER Fluid Squeeze Damper for Semi-active Vibration Control Devices: A Parametric Study", ASME Paper 95-GT-251.

Nelson, D. A., and Suydam, E. C., 1993, "The Thermal Aspects of the Electrorheological Effect and Its Impact on Application Design", FED-Vol. 164, Electro-Rheological Flows, ASME, pp.71-84.

Oyadiji, S. O., 1995, "Characterization of The Complex Shear Modulus Properties of Electro-Rheological Fluids by The Direct Stiffness and Master Curve Techniques", in Electro-Rheological Fluids, Magneto-Rheological Suspensions and Associated Technology, Prodeedings of the 5th International Conference Held in Sheffield, UK, 10-14 July 1995, edited by W. A. Bullough, World Scientific Publishing Co. Pte. Ltd., pp.419-428.

Petek, N. K., Goudie, R. J., Boyle, F. P., 1989, "Actively Controlled Damping in Electrorheological Fluid-Filled Engine Mounts". In *Electrorheological Fluids:* Proceedings of the Second International Conference on ER Fluids Held in Raleigh, North Carolina, August 7-9, 1989, edited by J. D. Carlson, A. F. Sprecher and H.Conrad, Lancaster: Technomic Publishing Co., pp. 409-418

Reitz, J. R. and Milford, F. J., 1967, Foundations of Electromagnetic Theory, Addison-Wesley Publication Company, Inc., pp. 106

Shulman, Z. P., 1982, "Utilization of Electric and Magnetic Fields for Control of Heat and Mass Transfer in Dispersed Systems", Heat Transfer-Soviet Research, Vol. 14, No.5, September-October (1982), pp. 1-23.

Shulman, Z. P., Zaltsgendler, E.A. and Gleb, V.K., 1986, Int. Heat Transfer Conference, Paper HX-31, pp. 367-372.

Shulman, Z. P., Novichyonok L.N., Belskaya, E.P., Khusid, B.M., and Melnichenko, V. V., 1982, "Thermal Conductivity of Metal-filled Systems", Int. J. Heat Mass Transfer, Vol. 25, No. 5, pp. 643-651.

Stangroom, J. E., 1983, Phys. Technol. 14: 290.

Tye, R. P., 1969, "Thermal Conductivity", Volume 2, Academic Press Inc., London LTD.

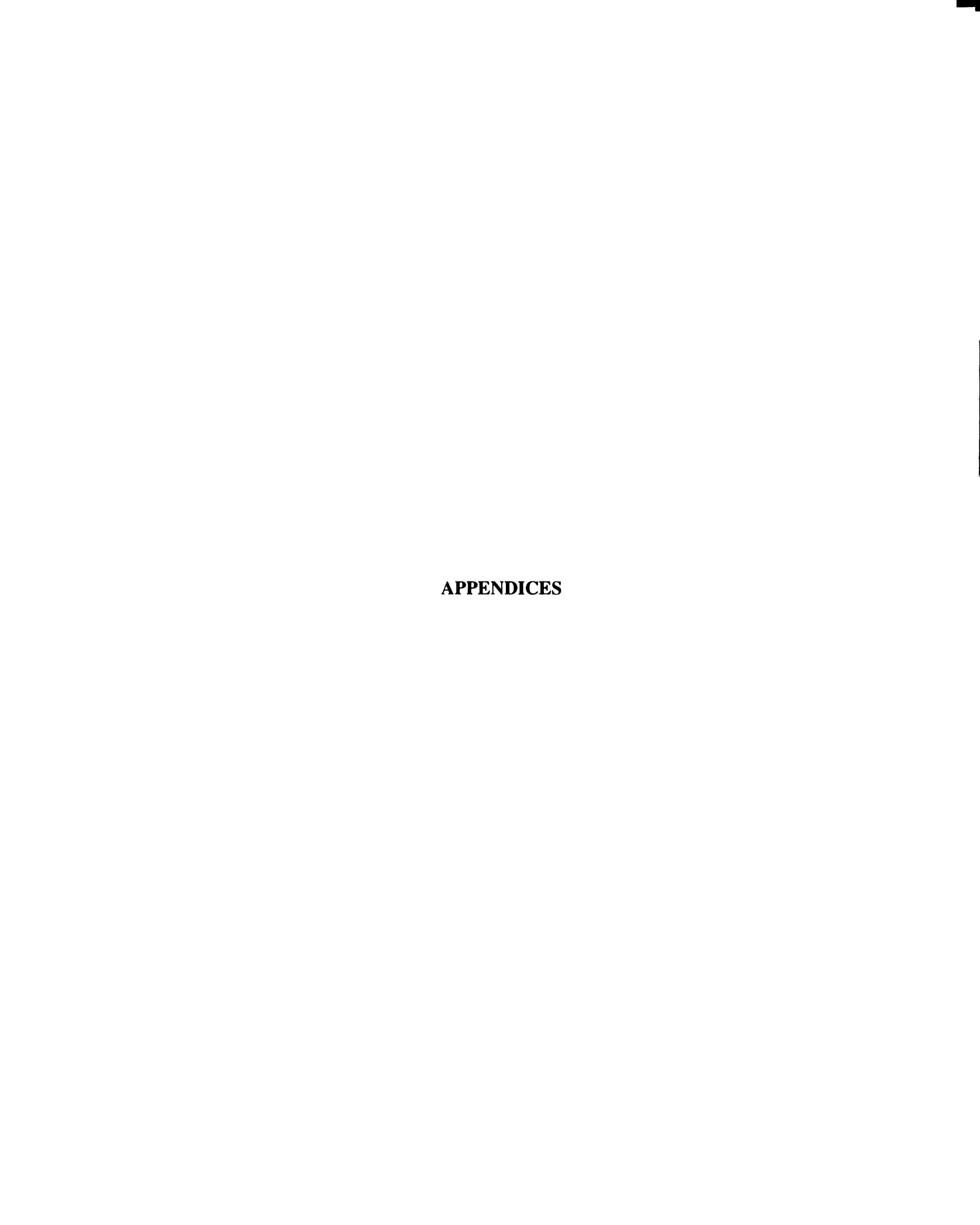
Williams, E. W., Rigby, S. G., Sproston, J. L., and Stanway, R., 1993, "Electrorheological Fluids Applied to an Automotive Engine Mount", Journal of Non-Newtonian Fluid Mechanics, Vol. 47, pp. 221-238.

Winslow, W. M., 1947, U. S. Patent 2, 417, 850

Zhang, C. and Lloyd, J. R., 1992, "Measurement of Radiation Heat Transfer in Electrorheological Fluid Based Composite Materials", *Developments in Radiative Heat Transfer*, HTD, Vol. 20, 1992 National Heat Transfer Conference, San Diego, CA, Aug. 8-11, pp. 55-62.

Zhang, C. and Lloyd, J. R., 1992, "A Numerical Investigation of Flow and Heat Transfer in a Thermosyphon Circulating ER Fluids", presented at the 4th Intl. Conf. on Electrorheological Fluids.

Zhang, C. and Lloyd, J. R., 1993, "Enhancement of Conduction Heat Transfer Through an Electrorheological Fluid Based Composite Medium", Fundamentals of Heat Transfer in Electromagnetic, Electrostatic and Acoustic Fields, HTD, Vol. 248, pp. 75-82.



APPENDIX A

Table 4 List of Available ER fluids

Piezoceramic

Sulphopropyl dextran

Particles	Suspending Fluid	
Corn Flour	Silicone oil	
Corn Starch	Corn oil	
Starch	Transformer oil	
Zeolite	Mineral Oil	
Zeolite	Hydrocarbon oil	
Carbon	Transformer oil	
Cellulose particles	Silicone oil	
Diatomaceous Earth	Engine oil	
Lime	Mineral oil	
Silica	Kerosene	
Sodium Carboxymethyl Cellulose	Silicone oil	
Gelatine	Olive oil	
LCP solution		
Glass Beads	Silicone oil	
Soft Ployurethane Particles	Silicone oil	
Poly (P-phenylene-2,	Mineral oil	
6-benzobisthiazole) [PBZ] PBZT		
Aluminum dihydrogen	Mineral oil	
Copper Phthalocyanine	Silicone oil	
Iron Oxide	Dibutyl sebacate	
_		

P-xylene Polychlorinated biphenyls

Table 5 General Characteristics of ER fluids (Gast and Zukoski 1989):

Suspending Fluid Properties

Relative Dielectric Constant $\varepsilon_f = 2-15$

Low Field Strength Conductivity $\sigma_f = 10^{-7} - 10^{-13} \text{ mho/m}$

Viscosity $\eta_f = 2-15$

Density $\rho_f = 10^{-7} - 10^{-13} \text{ mho/m}$

Particle Properties

Shape close to cubic or spherical

Size $a=0.1\text{-}100\mu m$

Relative Dielectric Constant $\varepsilon_p = 2-40$

Suspension Properties

Zero Field Viscosity $\eta_s = 10^{-7} - 10^{-13} \text{ mho/m}$

Volume Fraction of Particles $f_v = 0.05-0.5$

Electric Conductivity $\sigma_s = 10^{-6} - 10^{-13} \text{ mho/m}$

Typical Field Strength E = 0.1-5 kV/mm

Table 6 Data for Fig.8

Test	Steady State Method	Transient Method
1	0.13±0.008	0.139±0.0070
2	0.14±0.010	0.139±0.0070
3	0.14±0.011	0.140±0.0070
4		0.143±0.0072
5		0.136±0.0068

Table 7 Data for Fig.9

f _v	Eq. (2.1)	Eq. (2.4)	Eq. (2.5)	Measurement
0.1	0.909	1.010	0.909	0.749±0.0374
0.2	0.824	1.046	0.824	1.050±0.0525
0.25	0.783	1.077	0.783	1.036±0.0518
0.3	0.743	1.116	0.743	1.070±0.0535
0.35	0.667	1.167	0.704	1.164±0.0582
0.4	0.630	1.231	0.666	1.041±0.0520
0.45	0.595	1.308	0.629	

Table 8 Data for Fig.10

temperature (°C)	f _v = 35% water wt.8%	f _v =5% water wt.9%
24	0.156±0.0078	
25		0.121±0.0061
27	0.157±0.0079	
34		0.113±0.0057
37	0.131±0.0066	
40	0.119±0.0060	0.087±0.0044
42		0.086±0.0043
44	0.115±0.0058	
47	0.121±0.0061	
50	0.117±0.0059	0.083±0.0042

APPENDIX B

Experimental Uncertainty Analysis:

The experimental determination of any parameter is based upon measurements which by their nature contain errors. For the apparatuses considered in this study, the uncertainty errors are due to the inability to read a measurement device exactly. Utilizing a specific example we consider the experimental determination for the thermal conductivity, λ . This determination is based upon measurements of j, E, L, T_{0i} , T_{Li} based on equation (3.7) or the equation listed here

$$\lambda = \frac{jEL^2}{2\Delta T} \tag{1}$$

Then mathematically we have

$$Error = \left[\left(\frac{\partial \lambda}{\partial j} \delta j \right)^2 + \left(\frac{\partial \lambda}{\partial E} \delta E \right)^2 + \left(\frac{\partial \lambda}{\partial L} \delta L \right)^2 + \left(\frac{\partial T}{\partial \Delta T} \delta \Delta T \right)^2 \right]^{1/2}$$
 (2)

where the δ parameter represents the variation observed for each specific measurement, and

$$\frac{\partial \lambda}{\partial j} = \frac{EL^2}{2\Delta T}$$

$$\frac{\partial \lambda}{\partial E} = \frac{jL^2}{2\Delta T}$$

$$\frac{\partial \lambda}{\partial L} = \frac{jEL^2}{\Delta T}$$

$$\frac{\partial \lambda}{\partial \Delta T} = -\frac{jEL^2}{2\Delta T^2}$$
(3)

Since

$$E = \frac{V}{L}$$

then

$$Error_{E} = \left[\left(\frac{\partial E}{\partial V} \delta E \right)^{2} + \left(\frac{\partial E}{\partial L} \delta L \right)^{2} \right]^{1/2}$$

$$= \left[\left(\frac{\delta V}{L} \right)^{2} + \left(-\frac{V}{L^{2}} \delta L \right)^{2} \right]^{1/2}$$
(4)

Similarly,

$$j = \frac{4}{\pi} \frac{I}{D^2}$$

$$Error_{j} = \left[\frac{\partial j}{\partial I}\delta I\right]^{2} + \left(\frac{\partial j}{\partial D}\delta D\right)^{2}]^{1/2}$$

$$= \left[\left(\frac{4}{\pi}\frac{1}{D^{2}}\right)^{2} + \left(-\frac{2}{\pi}\frac{I}{D^{3}}\delta D\right)^{2}\right]^{1/2}$$
(5)

$$\Delta T = T_{0i}$$
,- T_{li}

$$Error_{\Delta T} = \left[\left(\frac{\partial \Delta T}{\partial T_{0i}} \delta T_{0i} \right)^2 + \left(\frac{\partial \Delta T}{\partial T_{Li}} \delta T_{Li} \right)^2 \right]^{1/2}$$
 (6)

The variations for the data in Table 3 are shown in Table 9.

Table 9 Values of Parameters and Their Variations

Parameter	Value	Variation
Current (I)	0.30 (mA)	0.005 (mA)
Voltage (V)	400 (V)	0.5 (V)
Temperature (T _{0i})	29 (°C)	0.005 (°C)
Temperature (T _{Li})	28.5 (°C)	0.005 (°C)
Thickness of ER	1.6 (mm)	0.05 (mm)
Fluid Layer (L)		

Using these values and equations (1) \sim (6) the error associated with the determination of a thermal conductivity of 0.28 W/mK can be estimated as 0.05 W/mK, which is in an error level of $\pm 11\%$. The errors for other measurements are estimated by the similar calculation.

MICHIGAN STATE UNIV. LIBRARIES
31293015638962